

## CYX X-3: A GALACTIC DOUBLE BLACK HOLE OR BLACK HOLE-NEUTRON STAR PROGENITOR

KRZYSZTOF BELCZYNSKI<sup>1,2</sup>, TOMASZ BULIK<sup>1</sup>, ILYA MANDEL<sup>3</sup>, B.S. SATHYAPRAKASH<sup>4</sup>, ANDRZEJ ZDZIARSKI<sup>5</sup>, JOANNA MIKOLAJEWSKA<sup>5</sup>

<sup>1</sup> Astronomical Observatory, University of Warsaw, Al. Ujazdowskie 4, 00-478 Warsaw, Poland

<sup>2</sup> Center for Gravitational Wave Astronomy, University of Texas at Brownsville, Brownsville, TX 78520, USA

<sup>3</sup> School of Physics and Astronomy, University of Birmingham, Edgbaston, B15 2TT, UK

<sup>4</sup> School of Physics and Astronomy, Cardiff University, 5, The Parade, Cardiff, UK, CF24 3YB

<sup>5</sup> Nicolaus Copernicus Astronomical Center, PAN, ul. Bartycka 18, 00-716 Warsaw, Poland

*Draft version November 11, 2018*

### ABSTRACT

There are no known double black hole (BH-BH) or black hole-neutron star (BH-NS) systems. We argue that Cyg X-3 is a very likely BH-BH or BH-NS progenitor. This Galactic X-ray binary consists of a compact object, wind-fed by a Wolf-Rayet (WR) type companion. Based on a comprehensive analysis of observational data, it was recently argued that Cyg X-3 harbors a 2–4.5  $M_{\odot}$  black hole (BH) and a 7.5–14.2  $M_{\odot}$  WR companion. We find that the fate of such a binary leads to the prompt ( $\lesssim 1$  Myr) formation of a close BH-BH system for the high end of the allowed WR mass ( $M_{\text{WR}} \gtrsim 13 M_{\odot}$ ). For the low- to mid-mass range of the WR star ( $M_{\text{WR}} \sim 7\text{--}10 M_{\odot}$ ) Cyg X-3 is most likely (probability 70%) disrupted when WR ends up as a supernova. However, with smaller probability, it may form a wide (15%) or a close (15%) BH-NS system. The advanced LIGO/VIRGO detection rate for mergers of BH-BH systems from the Cyg X-3 formation channel is  $\sim 10 \text{ yr}^{-1}$ , while it drops down to  $\sim 0.1 \text{ yr}^{-1}$  for BH-NS systems. If Cyg X-3 *in fact* hosts a low mass black hole and massive WR star, it lends additional support for the existence of BH-BH/BH-NS systems.

*Subject headings:* binaries: close — stars: evolution, neutron stars — gravitation

### 1. INTRODUCTION

Ever since the discovery of the Hulse-Taylor pulsar 1913+16 (Weisberg & Taylor 2005), a system consisting of a pair of neutron stars, there has been a lot of effort to detect other double compact objects. So far only double neutron star (NS-NS) systems were found (e.g., Lorimer 2008). In particular, no BH-NS nor BH-BH systems are known at the moment.

Merging compact binaries have provided the strongest motivation yet to build wide-band interferometric gravitational wave detectors. Second generation detectors, the Laser Interferometer Gravitational-wave Observatory (LIGO) in the US (Harry, 2010), Virgo in Italy (Acernese et al., 2006) and KAGRA (KAGRA 2012) in Japan, have the potential to observe the late inspiral and merger phases of compact binaries with their total mass in the range  $\sim [1, 10^3] M_{\odot}$ . The range of masses they could observe is determined by the frequency window of  $\sim [10, 10^4]$  Hz in which they operate. Radio binary pulsars lend strong motivation for systems at the lower end of the above mass range. When LIGO, Virgo and KAGRA begin their observations later in this decade, they could well provide the observational evidence for BH-NS/BH-BH systems or set very strong constraints on the statistics of their populations. However, we now have a plausible progenitor of a BH-NS/BH-BH system in our own galaxy.

High mass X-ray binaries (HMXBs) provide a unique opportunity to study various astrophysical phenomena. At *Warsaw Observatory* we have undertaken a program to study HMXBs in the context of the formation of double compact objects like BH-BH or BH-NS systems. We have already provided studies of two extragalactic HMXBs that

host the most massive known BHs of stellar origin: IC10 X-1 and NGC 300 X-1 (Bulik, Belczynski & Prestwich 2011), an analysis of Cyg X-1 binary that harbors the most massive stellar BH in our Galaxy (Belczynski, Bulik & Bailyn 2011) and analyses of several other binaries with well established parameters: GX 301-2, Vela X-1, XTEJ1855-026, 4U1907+09, Cir X-1, LMC X-1, LMC X-3, M33 X-1 (Belczynski, Bulik & Fryer 2012b).

In this study, we follow the recent estimate of system parameters for another Galactic HMXB: Cyg X-3. Zdziarski, Mikolajewska & Belczynski (2012) have estimated that Cyg X-3 consists of a low mass BH, 2–4.5  $M_{\odot}$ , and a massive WR star, 7.5–14.2  $M_{\odot}$ . We use this estimate to calculate the future evolution of Cyg X-3 to check whether this binary may provide any observational constraints on as-yet undetected BH-BH and BH-NS systems. The past evolution of Cyg X-3 was studied in detail by Lommen et al. (2005).

### 2. ESTIMATES

#### 2.1. *The future evolution of Cyg X-3*

In this section we describe in detail Cyg X-3 evolutionary scenarios leading to the formation of a BH-BH or BH-NS system. For demonstration we choose extremes of the allowed mass range of BH and WR components:  $M_{\text{BH1}} = 2.0$  with  $M_{\text{WR}} = 7.5 M_{\odot}$  and  $M_{\text{BH1}} = 4.5$  with  $M_{\text{WR}} = 14.2 M_{\odot}$ . Additionally, we evolve the most likely configuration  $M_{\text{BH1}} = 2.4$  with  $M_{\text{WR}} = 10.3 M_{\odot}$  as adopted from Zdziarski et al. (2012). First, we employ our standard model for stellar and binary evolution (see below) and in the next section we will test how various evolutionary uncertainties change our results.

We evolve three  $M_{\text{zams}} = 27, 36, 50 M_{\odot}$  single stars (Hurley, Pols & Tout 2000) at solar metallicity  $Z = 0.02$  with our calibrated wind mass loss rates (Belczynski et al. 2010a). At  $t = 6.5, 5.2, 4.4$  Myr these stars leave the main sequence (MS) and become Hertzsprung gap objects with helium core of  $M_{\text{WR},i} = 7.5, 10.3, 14.2 M_{\odot}$ , respectively. We expose this core right after MS and make them naked helium stars: massive WR objects. We pair these WR stars with  $M_{\text{BH}1} = 2.0, 2.4, 4.5 M_{\odot}$  BHs and create three binaries all with orbital period of  $P_{\text{orb}} = 4.8$  hr as observed for Cyg X-3. Such an approach allows a WR star to shed a maximum amount of mass, reducing its chance to become NS or BH, and thus makes our estimates conservative. We should note that this simplified picture in which the WR star is evolved independently of its companion ignores the effect of past interactions with the BH companion on the future evolution of the WR star, which could change the rate of future mass loss. However, the mass loss rates that we apply to WR companion are derived based on a large population of WR stars, including those in binaries (see below).

The binary separations at the currently observed orbital period of the three synthetic binaries are  $a = 3.0, 3.4, 3.8 R_{\odot}$  and the Roche lobe radii of WR component are  $R_{\text{lobe}} = 1.5, 1.7, 1.8 R_{\odot}$ . The corresponding radii of WR stars are  $R_{\text{WR}} = 0.8, 1.0, 1.2 R_{\odot}$ . Massive helium stars do not expand at any significant level during evolution. Therefore, no Roche lobe mass transfer episode is expected in the future evolution of these systems.

The lifetimes of these WR stars are  $t_{\text{life}} = 0.95, 0.77, 0.64$  Myr and at the end of their evolution the masses drop to  $M_{\text{WR},f} = 5.5, 6.8, 8.2 M_{\odot}$ . We have applied wind mass loss rates adopted from Hamann & Koesterke (1998) that take into account effects of clumping

$$(dM/dt) = 10^{-13} \left( \frac{L}{L_{\odot}} \right)^{1.5} M_{\odot} \text{ yr}^{-1}. \quad (1)$$

This prescription is based on detailed stellar evolutionary calculations combined with comprehensive WR wind models and calibrated on observations of three WR stars. We obtain WR star luminosity ( $L$ ) from evolutionary models of Hurley et al. (2000).

At the time of explosion, orbits have expanded to  $a = 3.9, 4.7, 5.6 R_{\odot}$  due to the WR wind mass loss and WR stars have formed massive CO cores ( $M_{\text{CO}} = 4.0, 5.0, 6.2 M_{\odot}$ ). The WR stars undergo a core collapse. We use Fryer et al. (2012) rapid explosion model that reproduces the observed mass gap between neutron stars and black holes (Belczynski et al. 2012a). For initial  $M_{\text{WR},i} = 7.5, 10.3 M_{\odot}$  WR stars the core collapse is followed by Type Ib supernova and neutron stars form with mass  $M_{\text{NS}} = 1.5, 1.7 M_{\odot}$ , respectively. The mass loss and natal kicks associated with supernova are very likely to disrupt these two synthetic binaries ( $f_{\text{disruption}} = 0.69$ ). However, there is also a significant chance to form a close BH-NS system. We estimate the probability of the BH-NS system formation with gravitational merger time  $T_{\text{merger}}$  shorter than 10 Gyr at the level  $f_{\text{close}} = 0.14, 0.12$  for the low and intermediate mass realization of Cyg X-3. We have applied a distribution of natal kicks as derived from the population of Galactic pulsars (Hobbs et al. 2005). The kicks have a random direction and their magnitude is

taken from a single Maxwellian with  $\sigma = 265 \text{ km s}^{-1}$ . Additionally, we lower the magnitude of natal kicks due to the amount of fall back expected in each supernova explosion  $V_{\text{kick}} = (1 - f_{\text{fb}})V_{\text{kick}}$  (Fryer et al. 2012). The fall-back amount, the fraction of matter that was initially ejected in a supernova explosion but that is later accreted back onto the compact object, was estimated to be  $f_{\text{fb}} = 0.14, 0.16$  in case of models with initial  $M_{\text{WR},i} = 7.5, 10.3 M_{\odot}$ , respectively.

For the high component-mass realization ( $M_{\text{WR},i} = 14.2 M_{\odot}$ ), within our rapid supernova explosion model the entire WR star falls into a BH (i.e.,  $f_{\text{fb}} = 1.0$ ). We assume the loss of 10% of the gravitational mass during the collapse through neutrino emission, which leads to a slight orbital expansion and a small induced eccentricity ( $a = 6.0 R_{\odot}$ ,  $e = 0.07$ ). In the end the second BH forms with mass  $M_{\text{BH},2} = 7.4 M_{\odot}$ . No natal kick is imparted on a BH within this model. Therefore, a close BH-BH system forms with a chirp mass of  $M_{\text{c,dco}} \equiv (M_1 M_2)^{3/5} (M_1 + M_2)^{-1/5} = 5.0 M_{\odot}$  and a merger time of  $T_{\text{merger}} = 0.5$  Gyr. In this particular case with no natal kick there is no other possibility ( $f_{\text{close}} = 1.0$ ), within the framework of our model, then to form a close ( $T_{\text{merger}} < 10$  Gyr) BH-BH system.

If we conservatively assume that at any given time there is only 1 such system as Cyg X-3 it means that Galactic birth rate is at the level  $\mathcal{R}_{\text{birth}} = 1/t_{\text{WR}}$ . As listed above, lifetimes of the considered massive WR stars are very short  $t_{\text{WR}} \lesssim 1$  Myr. Since the merger times of systems that we include in our analysis are relatively short ( $T_{\text{merger}} < 10$  Gyr) and the star formation was approximately constant in the Galactic disk over a long period of time ( $\sim 10$  Gyr) the Galactic merger rate of BH-NS and BH-BH systems may be estimated from

$$\mathcal{R}_{\text{MW}} = f_{\text{close}} \mathcal{R}_{\text{birth}} \sim f_{\text{close}} \frac{1}{t_{\text{WR}}}; \quad (2)$$

we discuss statistical uncertainties in the estimate of the birth rates in section 2.4. For our three Cyg X-3 realizations we obtain  $\mathcal{R}_{\text{MW}} = 0.19, 0.20 \text{ Myr}^{-1}$  in the cases of BH-NS formation and  $\mathcal{R}_{\text{MW}} = 1.56 \text{ Myr}^{-1}$  in the case of BH-BH formation. The main results presented in this section are summarized in Table 1 (top 3 entries) and illustrated in Figure 1 (top panel).

## 2.2. Range of evolutionary uncertainties

Alternatively to our standard approach, we employ WR wind mass loss rates adopted from Zdziarski et al. (2012):

$$(dM/dt) = 1.9 \times 10^{-5} \left( \frac{M_{\text{WR}}}{14.7 M_{\odot}} \right)^{2.93} M_{\odot} \text{ yr}^{-1}. \quad (3)$$

Zdziarski et al. (2012) selected data points from Nugis & Lamers (2000) for WR stars of similar mass and type as the one in Cyg X-3. Nugis & Lamers (2000) have estimated clumping corrected mass loss rates based on observations and modeling of 64 Galactic WR stars. We refer to this wind mass loss prescription as empirical as it is heavily derived from observations in contrast to the method used in our standard approach (mostly originating from theoretical predictions). In particular Zdziarski et al. (2012) employed data points from Table 5 of Nugis & Lamers (2000) for WN stars. It is worth noting that the majority of these

WN stars (19 out of 34) are in binary systems. The results of calculations with those winds are presented in Table 1 (models marked with “Wind: empiri” entry) and in Figure 1 (bottom panel). It is noted that both wind mass loss prescriptions give very similar results. There are no significant changes in our analysis. There is only a slight increase of BH mass ( $M_{\text{BH}2} = 8.0 M_{\odot}$ ) in the case of BH-BH formation.

Next, we alternate our approach to natal kicks. We adopt high kicks for all compact objects. It means that both neutron stars and black holes receive the kicks from the same distribution described by a Maxwellian with  $\sigma = 265 \text{ km s}^{-1}$ . There is no kick decrease factor applied in this case. Results for such an approach are listed in Table 1 (marked with “Kicks: high” entry). There is no significant changes for the BH-NS formation, as neutron stars in our standard model analysis were receiving almost full kicks (low fall back). There is a noticeable decrease in the formation efficiency of close BH-BH systems ( $f_{\text{close}} = 0.68$ ) that leads to corresponding decrease in the Galactic merger rate ( $\mathcal{R}_{\text{MW}} = 1.06 \text{ Myr}^{-1}$ ). The decrease is caused by binary disruptions due to high natal kicks applied to black holes in this model. However, the formation efficiency is still significant despite the rather high kicks that black holes receive in this model, because the binary’s initial orbital velocity,  $\sim 800 \text{ km s}^{-1}$ , is already large compared with typical kicks.

Our calculations so far were based on the rapid supernova explosion engine, in which a sufficiently massive progenitor does not explode at all, gets no natal kick and forms quite massive black hole. In the rapid model this is the reason for the emergence of a mass gap between NS and BH masses (Belczynski et al. 2012a, although see Kreidberg et al. 2012). On the one hand, lower mass stars are subject to strong explosions and form neutron stars (as in case of  $M_{\text{WR}} = 7.5, 10.3 M_{\odot}$ ). On the other hand, higher mass stars do not explode at all and form massive black holes (as for  $M_{\text{WR}} = 14.2 M_{\odot}$ ). This explains the rather sharp transition for all models considered thus far from  $M_{\text{WR}} = 10.3 M_{\odot}$  forming a neutron star ( $M_{\text{NS}} = 1.7\text{--}1.8 M_{\odot}$ ) to  $M_{\text{WR}} = 14.2 M_{\odot}$  forming quite massive black hole ( $M_{\text{BH}2} = 7.4\text{--}8 M_{\odot}$ ).

As a final variant, we have modified our approach to supernovae explosions. We now use the delayed explosion model of Fryer et al. (2012). This model generates a continuous compact-object mass spectrum (i.e., without a mass gap). The results for this set of calculations are listed in Table 1 (marked with “SN: delayed” entry). Due to the delayed nature of the explosion engine, neutron stars are typically more massive as proto-neutron stars have more time for accretion between the core bounce and actual explosion. The explosions are also typically less energetic, since at later times, after some cooling, there is less energy to drive the explosion. This leads to two changes for BH-NS formation. First, there is a noticeable increase in the formation efficiency (lower explosion energy leads to increased fall back and smaller natal kicks). Second, we note a significant increase in the NS mass. In fact, for the most likely Cyg X-3 configuration ( $M_{\text{BH}1} = 2.4$ ;  $M_{\text{WR}} = 10.3 M_{\odot}$ ), instead of forming a NS ( $M_{\text{NS}} = 1.7\text{--}1.8 M_{\odot}$  in all other models), we obtain a low-mass black hole ( $M_{\text{BH}2} = 2.7 M_{\odot}$ ) and thus transition from BH-NS

to BH-BH formation. In the case of the Cyg X-3 high-mass configuration we predict as before the formation of a BH-BH binary. The black hole in this model is formed with moderate fall back ( $f_{\text{fb}} = 0.43$ ), and therefore receives a moderate natal kick. It has significantly lower mass ( $M_{\text{BH}2} = 3.9 M_{\odot}$ ), since the majority of the ejected material was not a subject to fall back. As a result, the formation efficiency is significantly decreased ( $f_{\text{close}} = 0.5$ ) relative to all other models. Figure 2 shows the mass of the final compact object as a function of the initial mass of the WR star for all alternative models considered in this section.

### 2.3. LIGO/VIRGO detection rate estimate

In order to compute the advanced LIGO/Virgo event rates, we use the same detection threshold that was adopted in (Abadie et al., 2010) – a signal-to-noise ratio (SNR) of 8 in a single interferometer at the sensitivity of advanced LIGO. This is a simplified treatment, since actual detector sensitivity will depend on the network configuration, data quality, and the details of the search pipeline, but the uncertainties introduced by this simplifying assumption are smaller than the uncertainties in the merger rates.

Previous calculations in the population-synthesis literature (e.g., Belczynski et al., 2010b) were based on a simple scaling of the detection volume for arbitrary systems with the horizon distance  $d_0$  for a NS-NS binary (the distance at which an optimally oriented source with component masses  $M_1 = M_2 = 1.4 M_{\odot}$  could be detected at an SNR of 8):

$$\mathcal{R}_{\text{LIGO}} = \rho_{\text{gal}} \frac{4\pi}{3} \left( \frac{d_0}{f_{\text{pos}}} \right)^3 \left( \frac{\mathcal{M}_{\text{c,dco}}}{\mathcal{M}_{\text{c,nsns}}} \right)^{15/6} \mathcal{R}_{\text{MW}}. \quad (4)$$

Here,  $\rho_{\text{gal}}$  is the density of Milky Way-like galaxies, the chirp mass  $\mathcal{M}_{\text{c,nsns}} \equiv M_1^{3/5} M_2^{3/5} (M_1 + M_2)^{-1/5} = 1.2 M_{\odot}$  and the correction factor  $f_{\text{pos}} = 2.26$  takes into account the non-uniform pattern of detector sensitivity and random sky location and orientation of sources (Finn, 1996).

However, this simple calculation suffered from several shortcomings. The sensitivity distance scales as  $d \sim d_0 (\mathcal{M}_{\text{c,dco}}/\mathcal{M}_{\text{c,nsns}})^{5/6}$  only for masses sufficiently low that the gravitational-wave signal spans the bandwidth of the detector. The waveforms used to compute the horizon distance included only the contribution from the inspiral portion, not the merger and ringdown signals. Finally, cosmological effects due to the expansion of the universe have not been included: the redshifting (dilation) of masses in the gravitational waveform; the difference between the volume as a function of luminosity distance  $d$  and comoving volume; and the difference in the rate of clocks in the source and merger frames. Here, we include these effects by using the following procedure when integrating over shells centered on the detector:

- For each shell at a given redshift  $z$ , compute the luminosity distance  $d(z)$  and the comoving volume of the shell  $dV_c(z)$  using standard cosmology (see, e.g., Hogg, 1999) with  $\Omega_M = 0.272$ ,  $\Omega_{\Lambda} = 0.728$ ,  $h = 70.4$  (WMAP 7 results).
- Given a particular combination of compact-object masses from Table 1, compute the SNR for an opti-

mally oriented source at distance  $d(z)$ ,

$$SNR^2 = 4 \int_0^\infty \frac{|\tilde{h}(f)|^2}{S_n(f)} df, \quad (5)$$

where we use the inspiral-merger-ringdown waveform family IMRPhenomB (Ajith, 2010) to compute the frequency-domain waveforms  $\tilde{h}(f)$  using redshifted component masses  $M \rightarrow M(1+z)$  and the zero-detuning, high-power Advanced LIGO noise power spectral density  $S_n(f)$ .

- Compute the fraction of detectable mergers  $f_{\text{det}}(z)$  from this shell by considering the fraction of sources for which the projection function  $\Theta(\iota, \theta, \psi, \phi)$  [given in Eqs. (3.4.b–d) of (Finn, 1996)] is large enough so that  $(\Theta/4)SNR \geq 8$ . The cumulative distribution function of  $\Theta$  can be computed numerically (the approximate expression given by Finn, 1996, not being sufficiently accurate) via a Monte Carlo over the inclination angle  $\iota$  (whose cosine is uniform in  $[0, 1]$ ), the sky-location spherical coordinates  $\theta$  (whose cosine is uniform in  $[0, 1]$ ) and  $\phi$  (uniform in  $[0, 2\pi]$ ), and polarization  $\psi$  (uniform in  $[0, \pi]$ ).
- The contribution of the shell to the detection rate is given by  $f_{\text{det}}(z)dV_c(z)\rho_{\text{gal}}\mathcal{R}_{\text{MW}}(1+z)^{-1}$ . We assume that the intrinsic merger rate in the source frame is independent of redshift (i.e., we don't include the redshift dependence of star formation rate or metallicity). Thus, we use  $\mathcal{R}_{\text{MW}}$  from Table 1, and scale it by the space density of Milky Way-like galaxies, for which we use 0.01 per  $\text{Mpc}^3$  of comoving volume. The final factor of  $1/(1+z)$  reflects the time dilation between the source clock, used to measure the merger rate, and the clock on Earth, used to measure the detection rate.

We can now integrate over multiple shells (or, in practice, compute an approximate Riemann sum over the shells numerically) to obtain the advanced LIGO/Virgo detection rates that we report in Table 1. Including merger and ringdown waveform phases and accounting for cosmological redshift corrections decreases the detected event rates by  $\gtrsim 15\%$  for BH-NS systems and by  $\gtrsim 30\%$  for BH-BH systems relative to the simple scaling of Eq. (4), largely because the comoving volume within a luminosity distance  $d$  is significantly smaller than  $(4/3)\pi d^3$  at non-trivial redshifts.

#### 2.4. Statistical uncertainty on merger and detection rates

We note that the rates derived above do not account for the statistical uncertainty associated with observing a single binary like Cygnus X-3. In practice, we do not know the exact rate from a single observation even if  $f_{\text{close}}$  and  $t_{\text{WR}}$  are known perfectly in Eq. 2. Assuming that the birth of binaries like Cygnus X-3 is a stochastic Poisson process with rate  $\mathcal{R}_{\text{birth}}$ , the probability of electromagnetically observing exactly one such system is

$$p(1 \text{ obs.} | \mathcal{R}_{\text{birth}}) = \mathcal{R}_{\text{birth}} t_{\text{WR}} \exp(-\mathcal{R}_{\text{birth}} t_{\text{WR}}). \quad (6)$$

We can compute the probability distribution on the rate given a single observation by using Bayes' theorem:

$$p(\mathcal{R}_{\text{birth}} | 1 \text{ obs.}) \propto p(\mathcal{R}_{\text{birth}}) p(1 \text{ obs.} | \mathcal{R}_{\text{birth}}), \quad (7)$$

where  $p(\mathcal{R}_{\text{birth}})$  is the prior probability on the birth rate of such systems.

If a flat prior is chosen,  $p(\mathcal{R}_{\text{birth}}) = \text{const}$ , the most likely birth rate is  $1/t_{\text{WR}}$ , the value used in Eq. 2. However, the 90% credible interval on the birth rate extends from  $0.35/t_{\text{WR}}$  (at the 5th percentile) to  $4.74/t_{\text{WR}}$  (at the 95th percentile).

Meanwhile, if an uninformative Jeffreys prior on the rate is chosen,  $p(\mathcal{R}_{\text{birth}}) \propto \mathcal{R}_{\text{birth}}^{-1/2}$ , the most likely birth rate is halved to  $1/2t_{\text{WR}}$ . The 90% credible interval is shifted downward to  $0.17/t_{\text{WR}} - 3.9/t_{\text{WR}}$ .

Finally, we can consider the case where we assume that there is *at least* one rather than *exactly* one binary in the Galaxy in the same stage as Cygnus X-3 (i.e., there may be other similar Galactic systems which have not been observed). In that case, we are interested in  $p(\mathcal{R}_{\text{birth}} | \geq 1 \text{ detection})$ , which scales with  $p(\geq 1 \text{ detection} | \mathcal{R}_{\text{birth}}) = 1 - \exp(-\mathcal{R}_{\text{birth}} t_{\text{WR}})$ . For the Jeffreys prior, the posterior birth rate distribution peaks at  $1.26/t_{\text{WR}}$ .

The merger rate in all cases is given by  $\mathcal{R}_{\text{MW}} = \mathcal{R}_{\text{birth}}/f_{\text{close}}$ , and so ranges by the same pre-factors relative to the rate given in Eq. 2. The large range of purely statistical uncertainty, which spans about a factor of 5 above and below the value in Eq. 2, reflects the difficulty of making robust inference from a single observation.

### 3. DISCUSSION

We have calculated the future evolution of Galactic binary Cyg X-3 harboring a compact object and a WR star. We have employed a recent Cyg X-3 component mass estimate from Zdziarski et al. (2012) and following their arguments we have assumed that the compact object in Cyg X-3 is a black hole.

Our results indicate that the future evolution and fate of Cyg X-3 is a strong function of mass of the WR star. Within the measurement uncertainties Cyg X-3 may either form a close BH-BH binary at the high end of the allowed WR mass ( $M_{\text{WR}} \sim 14 M_\odot$ ), or form a close BH-NS ( $\sim 15\%$ ), a wide BH-NS system ( $\sim 15\%$ ) or get disrupted producing single BH and NS ( $\sim 70\%$ ) at the low end and middle of the allowed mass range for the WR star ( $M_{\text{WR}} \sim 7-10 M_\odot$ ).

We have estimated the advanced LIGO/VIRGO detection rates in case of the close BH-BH and BH-NS formation. The rates are significant: in the case of BH-BH formation  $\mathcal{R}_{\text{LIGO}} \sim 10 \text{ yr}^{-1}$ . This is the first empirical estimate of a BH-BH detection rate based on a Galactic system. Previous empirical estimates were based on extragalactic high mass X-ray binaries in small star forming galaxies IC10 and NGC300 (Bulik et al. 2011). The predicted rates that are based on observations within Milky Way (high metallicity) are much lower than estimated for the above two low-metallicity galaxies. The BH-BH detection rate extrapolated from IC10 X-1 and NGC300 X-1 for advanced LIGO/Virgo is  $\mathcal{R}_{\text{LIGO}} \sim 2000 \text{ yr}^{-1}$ , where we used conservative mass estimates and mean merger rates from (Bulik et al. 2011) and converted merger rates to detection rates as discussed in section 2.3. The low metallicity environment can significantly boost close BH-BH formation rates as explained by Belczynski et al. (2010b).

The detection rate for BH-NS systems forming via the Cyg X-3 channel are low,  $\mathcal{R}_{\text{LIGO}} \sim 0.1 \text{ yr}^{-1}$ . However, our rates are only *lower limits* as more binaries similar to Cyg X-3 may currently exist in the local Universe and close BH-NS systems may potentially form via other formation channels. Among about  $\sim 200$  Galactic and extra-galactic high-mass X-ray binaries only a handful have established parameters (Liu, van Paradijs & van den Heuvel 2005, 2006) allowing for detection rate prediction (Belczynski et al. 2012b). Recent population synthesis calculations provide rates that are typically a few detections per year for BH-NS systems for advanced detectors (Dominik et al. 2012; Belczynski et al. 2012c). Our prediction is only the second empirical estimate for BH-NS detection rates. The first one was obtained for another Galactic system Cyg X-1 (Belczynski et al. 2011). We note that our current rate ( $\sim 1$  detection per decade) is 10 times higher than the one obtained for Cyg X-1 ( $\sim 1$  detection per century).

Beyond our standard evolutionary calculations we have performed several models to check the validity of our conclusions. We have varied WR wind mass loss rates, natal kicks that compact objects receive in supernovae, and the supernova explosion mechanism that alters the NS/BH mass spectrum. As long as we stay within the framework of rapid supernova explosion mechanism there are no significant changes to our conclusions. We find a range of detection rates  $\mathcal{R}_{\text{LIGO}} = 0.09\text{--}0.15 \text{ yr}^{-1}$  for BH-NS systems and  $\mathcal{R}_{\text{LIGO}} = 7.7\text{--}12.4 \text{ yr}^{-1}$  for BH-BH systems. Our standard supernova model, which employs rapid explosions, is

motivated by the existence of the mass gap between neutron stars and black holes (e.g., Bailyn 1998; Ozel et al. 2010; Farr et al. 2011). However, if the mass gap is not an intrinsic signature of the BH/NS mass spectrum but is caused by some observational bias as recently claimed by Kreidberg et al. (2012), our conclusions change. For the delayed supernova model, which is consistent with the absence of a mass gap, we find that BH-NS formation occurs only at the lowest allowed mass for the WR star in Cyg X-3 ( $M_{\text{WR}} \sim 7 M_{\odot}$ ) with a slightly higher detection rate  $\mathcal{R}_{\text{LIGO}} = 0.17 \text{ yr}^{-1}$ . BH-BH formation is found in a broader mass range allowed for the WR star ( $M_{\text{WR}} \sim 10\text{--}14 M_{\odot}$ ). The second BH falls right within the mass gap ( $M_{\text{BH2}} = 2.7\text{--}3.9 M_{\odot}$ ) and the rates are significantly smaller,  $\mathcal{R}_{\text{LIGO}} = 0.41\text{--}2.8 \text{ yr}^{-1}$ . Finally, we note that all merger and detection rates have statistical uncertainties of approximately a factor of 5 in either direction due to the limited observational sample of a single system.

Authors acknowledge support from MSHE grant N203 404939 (KB) and NASA Grant NNX09AV06A to the UTB Center for Gravitational Wave Astronomy (KB). AAZ acknowledges support from the Polish NCN grant N N203 581240 and TB support from 623/N-VIRGO/09/2010/0. KB, IM and BS acknowledge the hospitality of KITP, supported in part by the National Science Foundation under No. NSF Grant PHY11-25915.

## REFERENCES

- Abadie J., et al. 2010, *Classical and Quantum Gravity* 27, 173001  
 Acernese F., et al. 2006, *Class. and Quantum Grav.* 23, S635  
 KAGRA, Large-scale cryogenic gravitational-wave telescope project  
 URL <http://www.icrr.u-tokyo.ac.jp/gr/LCGT.html>  
 Bailyn, C., Jain, R., Coppi, P., & Orosz, J. 1998, *ApJ*, 499, 367  
 Belczynski, K., Bulik, T., Fryer, C., Ruiter, A., Valsecchi, F., Vink, J., & Hurley, J. 2010a, *ApJ*, 714, 1217  
 Belczynski, K., Dominik, M., Bulik, T., O’Shaughnessy, R., Fryer, C., Holz, D. 2010b, *ApJ*, 715, L138  
 Belczynski, K., Bulik, T., & Bailyn, C. 2011, *ApJ*, 742, L2  
 Belczynski, K., Wiktorowicz, G., Fryer, C., Holz, D., & Kalogera, V. 2012a, *ApJ*, accepted (arXiv:1110.1635)  
 Belczynski, K., Bulik, T., & Fryer, C. 2012b, *ApJ*, submitted (arXiv:1208.2422)  
 Belczynski, K., & Dominik, M. 2012c, *ApJ*, submitted (arXiv:1208.0358)  
 Bulik, T., Belczynski, K., & Prestwich, A. 2011, *ApJ*, 730, 140  
 Dominik, M., et al. 2012, *ApJ*, accepted (arXiv:1202.4901)  
 Ergma E., Yungelson L. R., 1998, *A&A*, 333, 151  
 Farr, W., et al. 2011, *ApJ*, accepted (arXiv:1011.1459)  
 Finn, L. S. 1996. *Phys. Rev. D* 53, 2878  
 Fryer, C., et al. 2012, *ApJ*, 749, 91  
 Hamann, W., & Koesterke, L. 1998, *A&A*, 335, 1003  
 Harry G. M. (for the LIGO Scientific Collaboration), 2010, *Class. Quantum Grav.* 27 084006  
 Hobbs, G., Lorimer, D., Lyne, A., & Kramer, M. 2005, *MNRAS*, 360, 974  
 Hogg, D. W. 1999. arXiv:astro-ph/9905116  
 Hurley, J., Pols, O., & Tout, C. 2000, *MNRAS*, 315, 543  
 Kreidberg L., Bailyn C., Farr W., & Kalogera V. 2012, *ApJ*, submitted (arXiv:1205.1805)  
 Liu, Q.Z., van Paradijs, J. & van den Heuvel, E.P.J. 2005, *A&A*, 442, 1135  
 Liu, Q.Z., van Paradijs, J. & van den Heuvel, E.P.J. 2006, *A&A*, 455, 1165  
 Lommen D., Yungelson L., van den Heuvel E., Nelemans G., Portegies Zwart S., 2005, *A&A*, 443, 231  
 Lorimer, D. 2008, *Living Reviews in Relativity*, 11, 8  
 Nugis, T., & Lamers H. 2000, *A&A*, 360, 227  
 Ozel, F., et al. 2010, *ApJ* 725, 1918  
 Weisberg J. M. & Taylor J. H. 2005, *ASP Conf. Ser.* 328, 25  
 Zdziarski, A., Mikolajewska, J., & Belczynski, K. 2012, *MNRAS*, submitted (arXiv:1208.5455)

TABLE 1  
THE FATE OF CYG X-3

$M_{\text{BH}} + M_{\text{WR}}$	Wind <sup>a</sup> /Kicks <sup>b</sup> /SN <sup>c</sup>	Outcome <sup>d</sup>	$f_{\text{close}}^e$	$M_{\text{c,dco}}$	$t_{\text{WR}}$	$\mathcal{R}_{\text{MW}}$	$\mathcal{R}_{\text{LIGO}}$
2.0 + 7.5 $M_{\odot}$	theory/low/rapid	BH-NS (2.0 + 1.5 $M_{\odot}$ )	0.18	1.5 $M_{\odot}$	0.95 Myr	0.19 Myr <sup>-1</sup>	0.09 yr <sup>-1</sup>
2.4 + 10.3 $M_{\odot}$	theory/low/rapid	BH-NS (2.4 + 1.7 $M_{\odot}$ )	0.15	1.8 $M_{\odot}$	0.77 Myr	0.20 Myr <sup>-1</sup>	0.13 yr <sup>-1</sup>
4.5 + 14.2 $M_{\odot}$	theory/low/rapid	BH-BH (4.5 + 7.4 $M_{\odot}$ )	1.00	5.0 $M_{\odot}$	0.64 Myr	1.56 Myr <sup>-1</sup>	11.3 yr <sup>-1</sup>
2.0 + 7.5 $M_{\odot}$	empiri/low/rapid	BH-NS (2.0 + 1.5 $M_{\odot}$ )	0.18	1.5 $M_{\odot}$	0.95 Myr	0.19 Myr <sup>-1</sup>	0.09 yr <sup>-1</sup>
2.4 + 10.3 $M_{\odot}$	empiri/low/rapid	BH-NS (2.4 + 1.8 $M_{\odot}$ )	0.15	1.8 $M_{\odot}$	0.76 Myr	0.20 Myr <sup>-1</sup>	0.14 yr <sup>-1</sup>
4.5 + 14.2 $M_{\odot}$	empiri/low/rapid	BH-BH (4.5 + 8.0 $M_{\odot}$ )	1.00	5.2 $M_{\odot}$	0.64 Myr	1.57 Myr <sup>-1</sup>	12.4 yr <sup>-1</sup>
2.0 + 7.5 $M_{\odot}$	theory/high/rapid	BH-NS (2.0 + 1.5 $M_{\odot}$ )	0.19	1.5 $M_{\odot}$	0.95 Myr	0.20 Myr <sup>-1</sup>	0.09 yr <sup>-1</sup>
2.4 + 10.3 $M_{\odot}$	theory/high/rapid	BH-NS (2.4 + 1.7 $M_{\odot}$ )	0.17	1.8 $M_{\odot}$	0.77 Myr	0.22 Myr <sup>-1</sup>	0.15 yr <sup>-1</sup>
4.5 + 14.2 $M_{\odot}$	theory/high/rapid	BH-BH (4.5 + 7.4 $M_{\odot}$ )	0.68	5.0 $M_{\odot}$	0.64 Myr	1.06 Myr <sup>-1</sup>	7.7 yr <sup>-1</sup>
2.0 + 7.5 $M_{\odot}$	theory/low/delayed	BH-NS (2.0 + 1.9 $M_{\odot}$ )	0.26	1.7 $M_{\odot}$	0.95 Myr	0.27 Myr <sup>-1</sup>	0.17 yr <sup>-1</sup>
2.4 + 10.3 $M_{\odot}$	theory/low/delayed	BH-BH (2.4 + 2.7 $M_{\odot}$ )	0.28	2.2 $M_{\odot}$	0.77 Myr	0.36 Myr <sup>-1</sup>	0.41 yr <sup>-1</sup>
4.5 + 14.2 $M_{\odot}$	theory/low/delayed	BH-BH (4.5 + 3.9 $M_{\odot}$ )	0.50	3.6 $M_{\odot}$	0.64 Myr	0.78 Myr <sup>-1</sup>	2.8 yr <sup>-1</sup>

<sup>a</sup> Either theoretically (eq. 1) or empirically (eq. 3) based WR wind mass loss rates are applied.

<sup>b</sup> High: NS and BH kicks are taken from a Maxwellian with  $\sigma = 265 \text{ km s}^{-1}$ . Low: the high kicks are decreased proportionally to the amount of fall back for both NSs and BHs.

<sup>c</sup> Compact-object formation model: either via rapid supernovae (mass gap) or delayed supernovae (no mass gap).

<sup>d</sup> Type of binary formed followed by the mass of compact objects.

<sup>e</sup> We only count binaries that have formed with merger time shorter than 10 Gyr (others are disrupted or form wider systems).

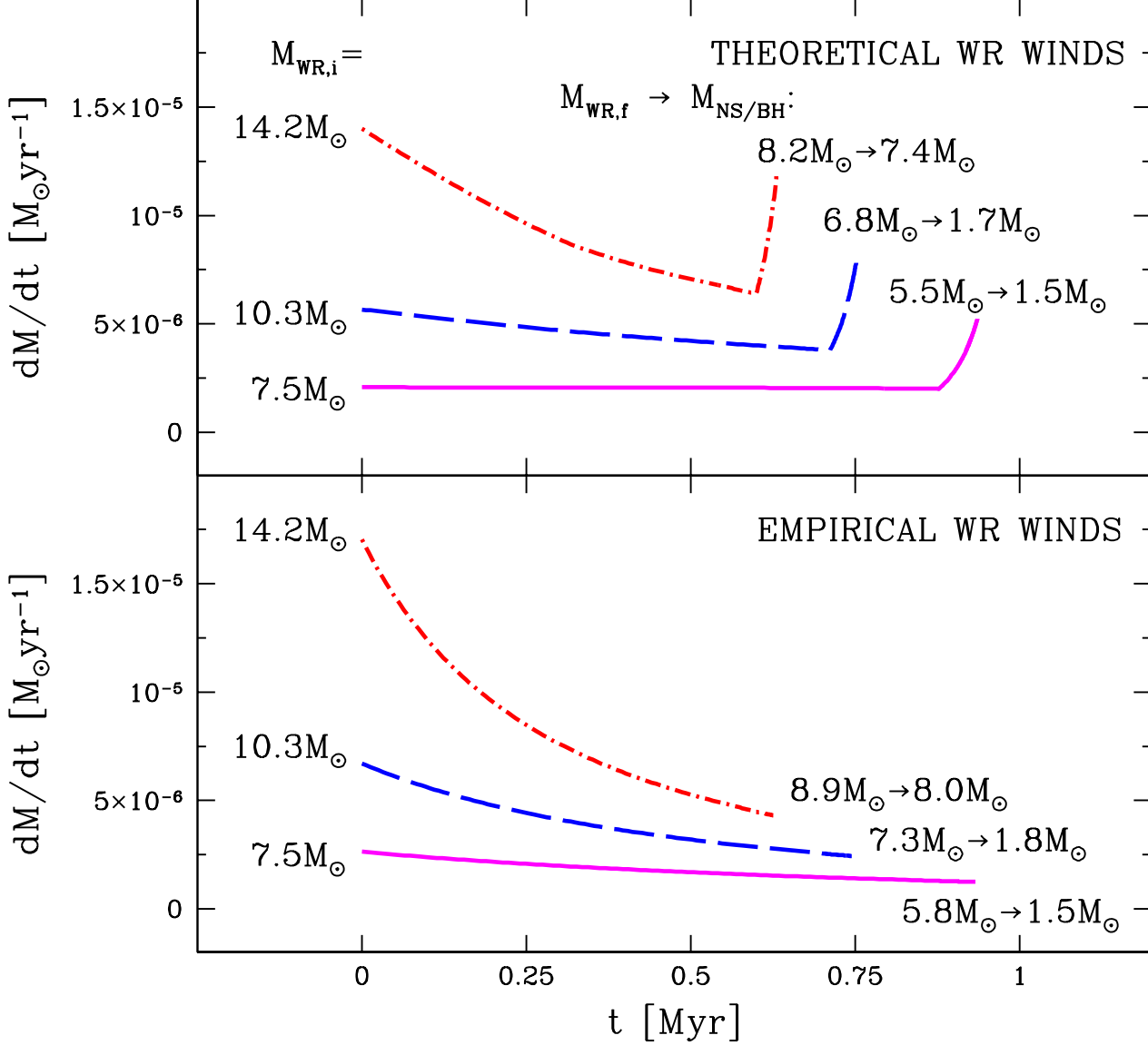


Fig. 1.— Evolutionary prediction for Cyg X-3 WR star ( $M_{\text{WR},i} = 10.3^{+3.9}_{-2.8} M_{\odot}$ ). Top panel shows the wind mass loss rate based on theoretical calculations, while results in bottom panel are based on observationally estimated WR mass loss rates. Independent of the adopted wind mass loss rate the WR component becomes either a neutron star for low- to medium-mass progenitors ( $M_{\text{WR},i} = 7.5\text{--}10.3 M_{\odot}$ ), and a black hole at the high end ( $M_{\text{WR},i} = 14.2 M_{\odot}$ ) of the allowed WR mass range. The mass of the WR component at the end of its evolution is marked with  $M_{\text{WR},f}$ , while the mass of compact object formed after core collapse/supernova explosion is marked with  $M_{\text{NS/BH}}$ . Compact objects with  $M_{\text{NS/BH}} < 2 M_{\odot}$  are assumed to be neutron stars, and above that black holes.

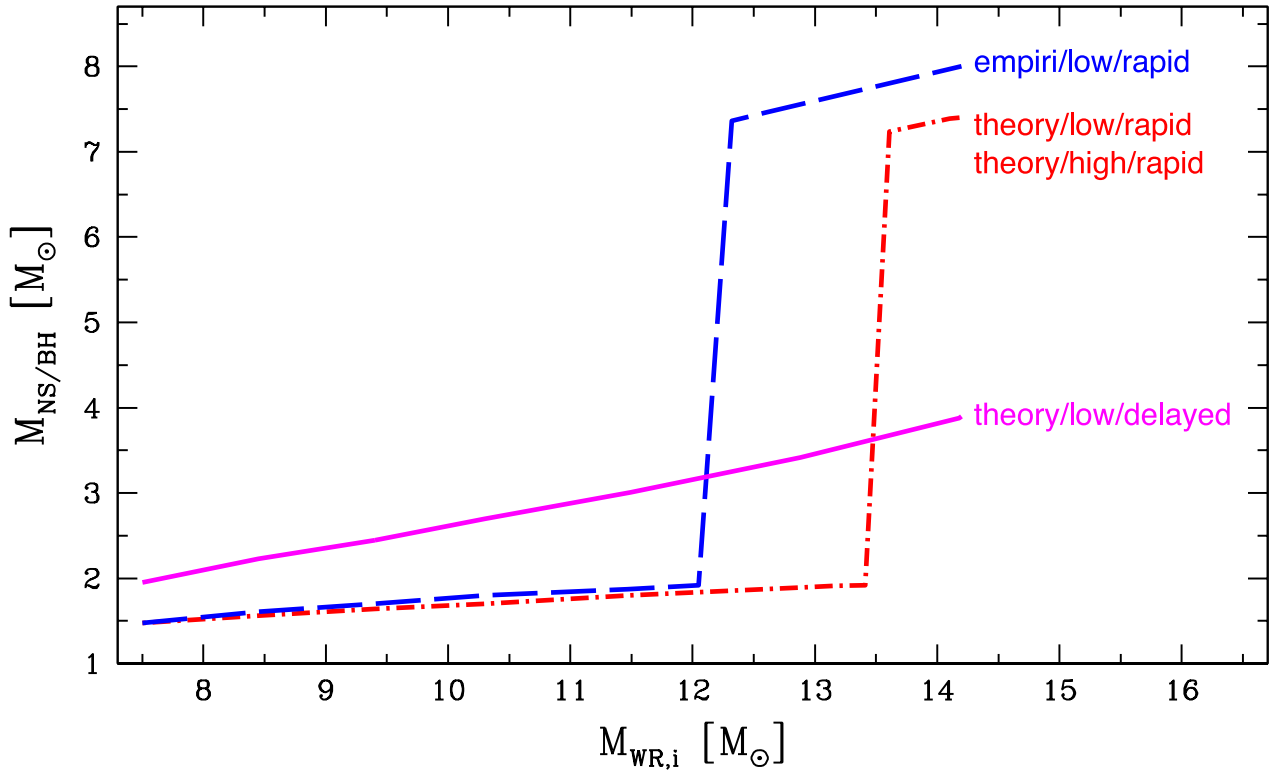


Fig. 2.— The dependence of the second compact object mass on the current WR star mass for Cyg X-3. There is a sharp transition from NS to BH formation for the rapid SN engine at around  $M_{\text{WR},i} \sim 12\text{--}13 M_{\odot}$ . The delayed SN engine allows for a steady increase of compact-object mass and the NS/BH transition depends sensitively on the unknown maximum NS mass. The assumed kick velocity has no impact on the compact-object mass, so two kick models (theory/low/rapid and theory/high/rapid) yield the same mass spectrum for the second compact object.